NMR spectroscopy of amino acid complexes of antimony(III) and indium(III) fluorides

V. Ya. Kavun, M. M. Polyantsev, L. A. Zemnukhova, and A. A. Udovenko*

Institute of Chemistry, Far Eastern Branch of the Russian Academy of Sciences, 159 pr. 100-letiya Vladivostoka, 690022 Vladivostok, Russian Federation. Fax + 7 (423) 231 1889. E-mail: kavun@ich.dvo.ru

The results of previously published NMR studies of amino acid complexes of antimony (III) and indium(III) fluorides are critically analyzed. Correlations between the NMR data, ion mobility, and structure of the complexes in question are considered. The interpretation of the low-temperature ^{19}F NMR spectra of amino acid complexes of antimony(III) fluorides is corrected and certain figures were changed for better informativity. Mechanisms of the onset of ion mobility in the studied complexes of Sb(III) and In(III) fluorides are proposed and the possibility of application of these compounds in the design of functional materials is assessed.

Key words: antimony(III) fluoride, indium(III) fluoride, amino acid, NMR spectra.

Introduction

Fundamental problems in present-day coordination chemistry include search for new compounds suitable for fabrication of functional materials based on them. Interest of researchers working in the field of design of advanced molecular materials is due to certain properties exhibited by amino acids (AA) in the formation of coordination compounds with metals. Amino acids can exist in three forms, *viz.*, as neutral zwitterionic molecules, protonated cations, and deprotonated anions. Comprehensive information on AA molecules as structural units of complexes with metal halides, which act as mono-, bi-, or tridentate ligands, can be found in a monograph.[1] The authors of that book emphasized a great variety of the crystal structures of the compounds in question and generalized the results of studies on the structure of molecular adducts with divalent metal halides. Recently, amino acid complexes of aluminum fluoride[2] and indium fluoride[3] have been reported for the first time. Information on the physicochemical properties of antimony(III) fluoride complexes with AA is scarce[4—7] in contrast to the data on homoligand complexes of antimony(III) fluorides with alkali metal, thallium(I), and ammonium cations. At present, there are a few publications on the synthesis, properties, and structure of antimony(III) fluoride and indium(III) fluoride complexes with organic cations and neutral molecules[8,9] and only one communication devoted to an indium(III) complex with AA.[3]

Antimony(III) fluoride is a good ion acceptor which forms numerous complexes.[10] Structural variety of complex compounds of antimony(III) fluorides underlies the onset of piezoelectric,[11] unusual electro-optical,[12,13] luminescence properties,[14] *etc*.[15,16] Besides, certain compounds undergo phase transitions (PT) to the superionic state with the conductivity in the range of nearly 10^{-4}—10^{0} S cm^{-1}.[12,16—20] Antimony trifluoride complexes with AA have been poorly studied. To date, antimony(III) fluoride complexes with glycine (Gly),[4,7] alanine (Ala),[21] valine (Val),[22] serine (Ser),[23] *etc*.[24—26] have been synthesized and their crystal structures determined. Carrying out X-ray phase analysis (XPA) as well as methods of investigation of structural and thermal properties, ion mobility, and conductivity of amino acid complexes of antimony(III) and indium(III) fluorides are well documented.[3,6,7,21—27] Stability of these compounds in aqueous solutions was also studied.[28]

Nuclear magnetic spectroscopy is an efficient method for investigation of the structure and properties of chemical compounds and functional materials.[29—32] It allows one to solve a broad spectrum of problems in studies of complexes of Group II—VI element fluorides with various ligands, including structure determination of complex anions, determination of the character of chemical bonds, PT, the dynamics of ion motions, *etc*. Scientific research in this field also involves studies on PT and ion mobility in the antimony(III) fluoride and indium(III) fluoride complexes with inorganic[17—19,33] and organic ligands.[3,6,7,27,34] An analysis of publications showed that most of them including out studies are devoted to the ion dynamics in complexes of antimony(III) fluorides with alkali metal cations and ammonium, whereas similar

* Based on the materials of the XXI Mendeleev Congress on General and Applied Chemistry (September 9—13, 2019, St. Petersburg, Russia).

Published in Russian in *Izvestiya Akademii Nauk. Seriya Khimicheskaya,* No. 9, pp. 1614—1624, September, 2020.

1066-5285/20/6909-1614

complexes of with AA received little attention until recently (except our publications[3,6,7,27]). The importance of NMR studies on the character of ion motions in solids is based on the possibility to directly separate the effects of rotational diffusion, which is not related to charge transfer, and translational diffusion of ions, which is responsible for the onset and magnitude of conductivity in the fluoride systems. The NMR data allow one to evaluate the conductivity of a system under study and to assess the prospects for further studies.

The present review is devoted to analysis of our studies on certain amino acid complexes of antimony(III) fluorides (with correction of results when necessary) and to correlations between the NMR data, ion mobility, and structure of the compounds in question. For comparison we use the ^{19}F NMR data for the sole indium(III) fluoride complex with amino acid.[3] The interpretation of the low-temperature ^{19}F NMR spectra of amino acid complexes of antimony(III) fluorides is revised. Mechanisms were proposed of the onset of ion mobility in the complexes studied and the possibility of their application for the design of functional materials was considered.

NMR spectroscopy of amino acid complexes of antimony(III) and indium(III) fluorides: data analysis and discussion

Methods for analysis of NMR data for particular compounds have been well documented.[3,6,7,27,35] Note that NMR spectra were simulated using a program that allows one to determine the second moments of the ^1H and ^{19}F NMR spectra ($S_2(H)$ and $S_2(F)$, respectively), full width at half maximum ($\Delta H_{1/2}$), chemical shifts (CS, δ) and the shape of spectral components, as well as the doublet splitting (Δ) value.

NMR data for antimony(III) fluoride complex with glycine $2SbF_3 \cdot (C_2H_5NO_2)$, $2SbF_3 \cdot Gly$

The observed shape of the ^{19}F NMR spectra (Fig. 1)[7] of the complex $2SbF_3 \cdot (C_2H_5NO_2)$ and a plateau on the temperature dependence $\Delta H_{1/2}(F) = f(T)$ (Fig. 2) suggests that no ion motions with frequencies higher than 10^4 Hz occur in the fluoride sublattice of the compound in the temperature range of 150—350 K (so-called "rigid lattice" according to solid-state NMR terminology).[30]

Assuming that the fluoride sublattice contains six fluorine atoms (3+3) from the nearest environment of two independent antimony(III) atoms and four fluorine atoms from the second coordination sphere (1+3), the ^{19}F NMR spectra of complex $2SbF_3 \cdot Gly$ at temperatures below 400 K were simulated[7] using two components, p_1 and p_2, with a relative integrated intensity (RII, in %) ratio of nearly 60 : 40%. However, an analysis of the Sb—F distances from the second coordination sphere (2.555 Å in the $Sb(1)F_4OE$ polyhedron and from 2.592 to 3.177 Å in the $Sb(2)F_4OE$ polyhedron, where E is the lone electron pair)[7] suggests that it is more logical and accurate to simulate the NMR spectra of complex $2SbF_3 \cdot Gly$ using two components, p_1 and p_2, with a RII ratio of 75 : 25 (Fig. 3). Taking account of positions of these spectral components, p_1 with CS = 130 ppm should be assigned to six fluorine atoms from the nearest environment of two antimony(III) atoms (Fig. 4) while p_2 with CS = 15 ppm

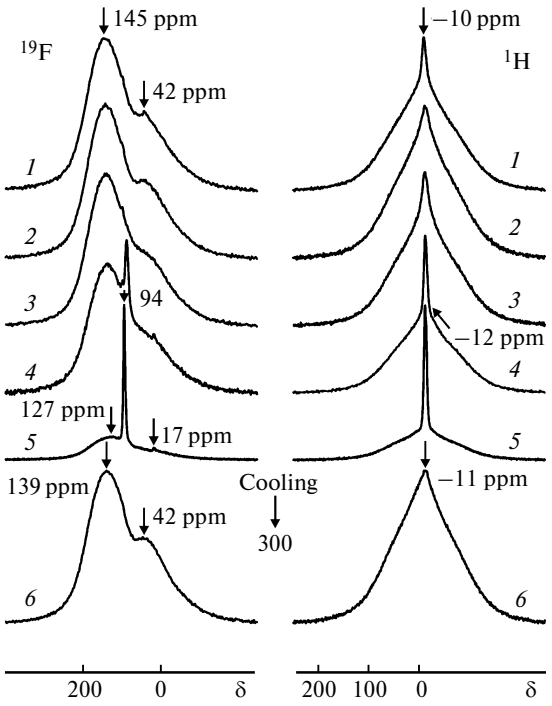

Fig. 1. ^1H NMR spectra (with Me_4Si as reference) and ^{19}F NMR spectra (with C_6F_6 as reference) of complex $2SbF_3 \cdot (C_2H_5NO_2)$ recorded at 300 (*1*), 370 (*2*), 400 (*3*) 420 (*4*), and 435 K (*5*) and on cooling from 435 to 300 K (*6*).

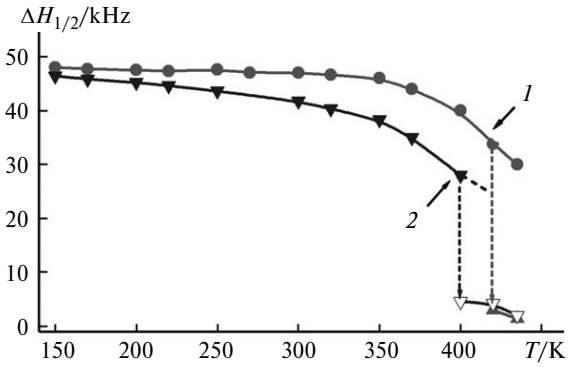

Fig. 2. Temperature dependences of half-width ($\Delta H_{1/2}$) ^{19}F NMR spectra (*1*) (activation energy $E_a = 0.66$ eV) and ^1H NMR spectra (*2*) ($E_a = 0.64$ eV) of compound $2SbF_3 \cdot (C_2H_5NO_2)$.

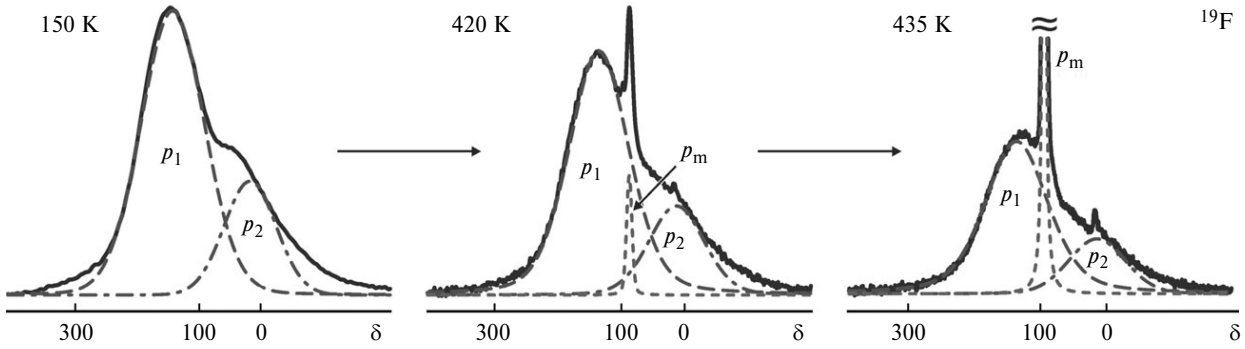

Fig. 3. Simulation of ^{19}F NMR spectra of compound $2SbF_3 \cdot (C_2H_5NO_2)$ at different temperatures (with C_6F_6 as reference).

corresponds to two bridging F atoms from the second coordination sphere of the antimony(III) atoms.

At temperatures above 400 K, the ^{19}F NMR spectrum of the complex exhibits a narrow line (p_m component) with CS = 95 ppm ($\Delta H_{1/2}$ = 2.8 kHz) corresponding to mobile fluorine ions. Taking account of the fact that the RII ratio of the p_1, p_2, and p_m components changes from 74.5 : 22.5 : 3.0 at 420 K to 62.5 : 16.5 : 21.0 at 435 K, one can assume that, initially, diffusion involves fluorine atoms from the second coordination sphere since the RII of p_m increases with increasing temperature due to a decrease in RII of p_2, and then other fluorine atoms are involved.

At T = 435 K, the half-width of the Lorentzian component p_m with CS = 95 ppm is 1.4 kHz (see Fig. 2), thus indicating intensification of translational diffusion involving to 21% of ions from the fluoride sublattice of the complex. Noteworthy is that position of the p_m component (with allowance for the error in the determination of the CS values for the broad spectral components p_1 and p_2 at low temperatures and for the contribution of the CS anisotropy to the overall spectrum) to a reasonable accuracy matches that of the "center of gravity" of the low-temperature NMR spectrum, $\langle\delta\rangle = 1/8(6 \cdot 130 + 2 \cdot 15) = 101$ ppm. It follows that fluorine atoms from not only the nearest environment of antimony atoms, but also the second coordination sphere are involved in fast intramolecular exchange at $T > 410$ K. These data are without doubt indicative of intramolecular dynamics between different ligands in the fluoride sublattice. Diffusion can occur as hopping of fluorine ions from one structural site to adjacent "free" site in the fluoride sublattice (thermal vacancy") that formed on heating the sample.[10] According to XPA and differential scanning calorimetry (DSC) data, the compound undergoes a PT with the formation of disordered crystalline phase at $T > 400$ K; this favors the onset of high ion mobility in both sublattices. Raising the temperature above 440 K is followed by melting of the sample and subsequent formation of X-ray amorphous phase on cooling.[7]

The NMR spectra shown in Figs 1 and 2 demonstrate that no ion motions with frequencies higher than 10^4 Hz occur in the proton sublattice ("rigid" lattice) in the temperature range of 150—350 K. "Triangular" shape of the ^{1}H NMR spectra of complex $2SbF_3 \cdot Gly$ at $150 \le T \le 270$ K (Fig. 5) results from superposition of the resonance lines p_1 and p_2 with a RII ratio of 59.8 : 39.9 = 1.49. The former line corresponds to the NH_2 group while the latter one (Pake doublet with the splitting $\Delta \approx 44 \pm 2$ kHz) corresponds to the CH_2 group in the glycine molecule ($NH_2 : CH_2 = 1.5$).

A narrow component p_m (4.6 kHz) appeared in the ^{1}H NMR spectrum of $2SbF_3 \cdot Gly$ at $T > 390$ K implies the presence of mobile protons (activation energy, E_a, of proton motions is nearly 0.64 eV). As the temperature increases to 435 K, the RII of this line increases to ~21%

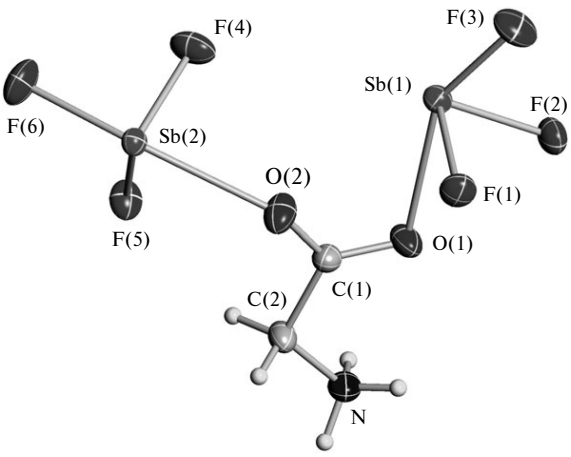

Fig. 4. Molecular structure of complex $2SbF_3 \cdot (C_2H_5NO_2)$.[7]

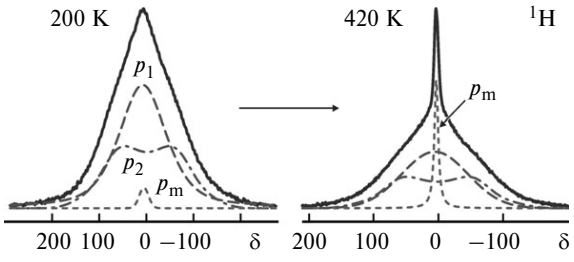

Fig. 5. Simulation of ^{1}H NMR spectra of compound $2SbF_3 \cdot (C_2H_5NO_2)$ at 200 and 420 K.

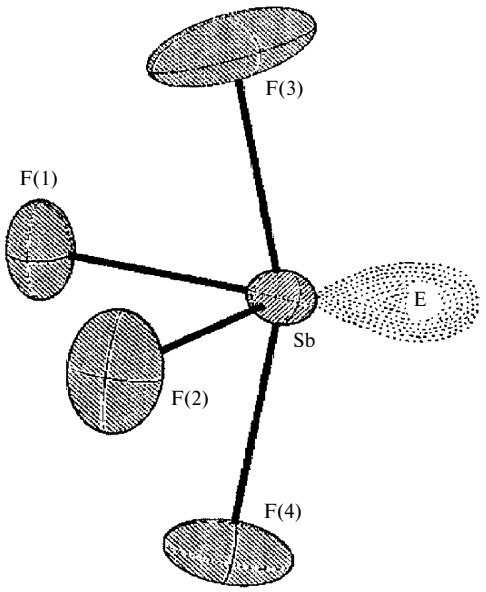

Fig. 6. Structure of complex anion $[SbF_4]^-$ in $(C_5H_{12}NO_2)SbF_4 \cdot H_2O$.

while the line narrows to 2 kHz ($S_2(H) \approx 0.14$ G^2); this suggests the development of diffusion in the proton subsystem of $2SbF_3 \cdot$Gly. An analysis of the RII of the components p_1 and p_2 (50.2 : 38.9) showed that the decrease in the RII of p_1 at constant RII of p_2 at $T = 420$ K is due to the involvement of amino group protons in the process.

As the temperature increases to 435 K, one cannot exclude the assumption that the mechanism of proton diffusion is related to proton exchange in the amino group due to fast reorientational motions of this group around the C(2)—N bond in the glycine molecule (see Fig. 4). A possible diffusion pathway includes proton migration over the crystal lattice.[36]

NMR data for compound $(C_5H_{12}NO_2)SbF_4 \cdot H_2O$, $(ValH)SbF_4 \cdot H_2O$

The coordination polyhedron of the Sb atom in (ValH)$SbF_4 \cdot H_2O$ is a ψ-trigonal bipyramid SbF_4E. Two fluorine atoms, F(1) and F(2), located at nearly equal distances from the Sb atom (1.922 and 1.939 Å, respectively), and the stereochemically active lone electron pair E of the Sb^{3+} ion lie in the equatorial plane (Fig. 6).[27] Axial vertices are occupied by the F(3) and F(4) atoms separated from the Sb atom by a distance of 2.042 and 2.131 Å, respectively. Taking into account the bridging atom F(3A) (Sb—F bond length 2.584 Å), the coordination polyhedron of the Sb(III) atom can be treated as ψ-tetragonal bipyramid SbF_5E with highly distorted equatorial plane. According to ^{19}F NMR data, no ion motions with frequencies higher than 10^4 Hz occur in $(ValH)SbF_4 \cdot H_2O$ in the temperature range of 150—400 K.

The ^{19}F NMR spectrum of the SbF_5E polyhedron was simulated[27] as superposition of four Gaussian components p_1, p_2, p_3, and p_4 (Fig. 7, *a*). They were assigned to the fluorine atoms F(1) + F(2); F(3); F(4), and F(3A) with allowance for their RII ratio (2 : 1 : 1 : 1). However, a more recent study revealed that incomplete averaging of the CS anisotropy in the ^{19}F MAS NMR spectrum (sample rotation frequency was varied from 12 to 16 kHz) allows one to deconvolve the spectrum into two components only. These components of different width with isotropic CS of −68 and −82 ppm can correspond to two equatorial fluorine atoms, F(1) + F(2), and two axial ones, F(3) + F(4), in the SbF_4E polyhedron. The error in the deconvolution of the spectrum into two components is more than halved (from 17 to 7.5%). It follows that deconvolution of the spectrum into four components is incorrect since the bridging atom F(3A) is a constituent of the other polyhedron, SbF_4E.

Deconvolution of the ^{19}F NMR spectra of the SbF_4E polyhedra into two components (Fig. 7, *b*) seems to be more realistic, although the effect of CS anisotropy is retained. It cannot be ruled out that the component corresponding to axial fluorine atoms is a close doublet since the Sb—F(3) and Sb—F(4) distances are different.

The change in the "center of gravity" of the NMR spectrum on going from the temperature range of 150—250 K to 300—420 K is apparently due to structural rearrangement of compound $(C_5H_{12}NO_2)SbF_4 \cdot H_2O$ upon a PT (endothermic effect at 351 K) followed by the formation

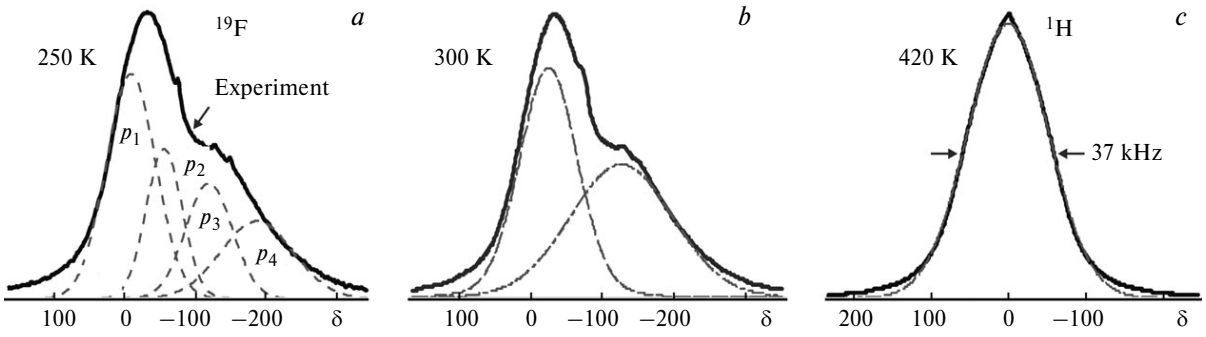

Fig. 7. Simulation of ^{19}F NMR spectra (*a*, *b*) and ^{1}H NMR spectra (*c*) of compound $(C_5H_{12}NO_2)SbF_4 \cdot H_2O$;[27] with CCl_3F (*a*, *b*) and Me_4Si (*c*) as references.

of X-ray amorphous phase. The dynamic state of fluorine ions characterized by the absence of translational and reorientational motions of these ions (Sb^{3+} polyhedra) is untouched by the process.

In the temperature range 150—420 K the ^{1}H NMR spectra of complex (ValH)$SbF_4 \cdot H_2O$ represent superpositions of lines from proton-containing groups in the $[(CH_3)_2(CH)_2(NH_3)(COOH)]^+$ cation and from water molecule (Fig. 7, *c*). Unchangeable shape and constant width of the ^{1}H NMR spectra upon temperature variation suggests that no ion motions with frequencies higher than 10^4 Hz occur in this compound in the temperature range studied. Attempts to deconvolve the ^{1}H NMR spectrum into components corresponding to particular groups in the cation and to H_2O molecule failed due to ambiguity and large error of simulation.

The absence of ion mobility in (ValH)$SbF_4 \cdot H_2O$ is most probably due to the presence of strong hydrogen bonds between NH_3 protons and COOH groups of the cation and water protons. These bonds fix the positions of fluorine ions and protons in the crystal lattice. In particular, there is a rather strong H-bond between the OH group and a fluorine atom of the SbF_4^- anion. The NH_3 group forms three relatively strong hydrogen bonds, two with F atoms and one with water oxygen atom; in turn, the H_2O molecule forms H-bonds with an oxygen atom of valinium cation and a fluorine atom.

NMR data for compound $(C_3H_8NO_3)Sb_2F_7$, $(SerH)Sb_2F_7$

According to ^{1}H NMR data for (SerH)Sb_2F_7, no motions occur in the proton sublattice of this compound in the temperature range of 150—200 K.[27] Judging by the chemical composition of the serinium cation, the ^{1}H NMR spectrum of (SerH)Sb_2F_7 in this temperature range (Fig. 8) should theoretically represent a superposition of at least four resonance lines from NH_3, CH_2, CH, and OH groups. Actually, the best results were obtained upon deconvolution of the NMR spectrum into three components p_1, p_2, and p_3 (the error was less than 15%). A qualitative analysis of the ^{1}H NMR spectra of (SerH)Sb_2F_7 in the temperature range of 150—210 K taking into account the lineshapes and the RII ratio of the spectral components equal to 49.5 : 25.0 : 25.5 (in %) showed that they can be assigned as follows: p_1 corresponds to HC—NH_3 groups, p_2 (Pake doublet) corresponds to CH_2 groups, and p_3 corresponds to 2OH groups (4:2:2) in the D,L-serinium cation $-[H_3N—CH—CH_2—OH—COOH]^+$.

A "narrow" spectral component p_m ($\Delta H_{1/2} \approx 7$ kHz) with a RII of nearly 8% (Fig. 8) observed at $T > 210$ K suggests the appearance of mobile protons ($E_a \approx 0.35$ eV). Its width and second moment are indicative of the development of ion diffusion in the compound.[30] Since this component is primarily (by about 80%) composed of a Gaussian function, one deals with orientational diffusion.[30] In the temperature range 220 → 320 K, the RII of the p_m component increases from about 8 to 53%, first of all, due to a decrease in the RII of the p_1 component corresponding to the HC—NH_3 group. One can assume that the appearance of mobile protons is related to fast intramolecular exchange between different atomic groups in the D,L-serinium cation. It is highly probable that protons from all groups are involved in diffusion, as indicated by the RII ratio of the components p_1, p_2, p_3, and p_m equal to 13 : 17 : 16 : 54 at 320 K compared to that at 200 K. At $T > 320$ K, dynamic processes in the proton subsystem of the complex (SerH)Sb_2F_7 precede an order—disorder PT (endothermic effect at 385 K). According to XPA data, the transition is followed by melting of (SerH)Sb_2F_7 and formation of X-ray amorphous phase (390 → 300 K).

From ^{19}F NMR data it follows that no ion motions with frequencies higher than 10^4 Hz occur in (SerH)Sb_2F_7 at $T < 250$ K (Fig. 9). Taking account of the structure of the complex anion (Fig. 10), the ^{19}F NMR spectrum at 170 K can tentatively be represented by the sum of three components p_1, p_2, and p_3 (RII ratio is 58 : 28 : 14) corresponding to four, two, and one fluorine atom, respectively. Based on the RII values, the p_3 component with CS ≈ −207 ppm can be assigned to the bridging fluorine atom F(4), the p_2 component with CS = −120 ppm corresponds to the axial atoms F(3) and F(7), while the p_1 component with CS = −7 ppm corresponds to other fluorine atoms F(1), F(2), F(5), and F(6) (see Figs 9 and 10).

A new line p_m in the simulated ^{19}F NMR spectrum ($\Delta H_{1/2}$(F) = 6.5 kHz, CS = −68 ppm) has a RII of 4% at 270 K (see Fig. 9) and corresponds to the appearance of

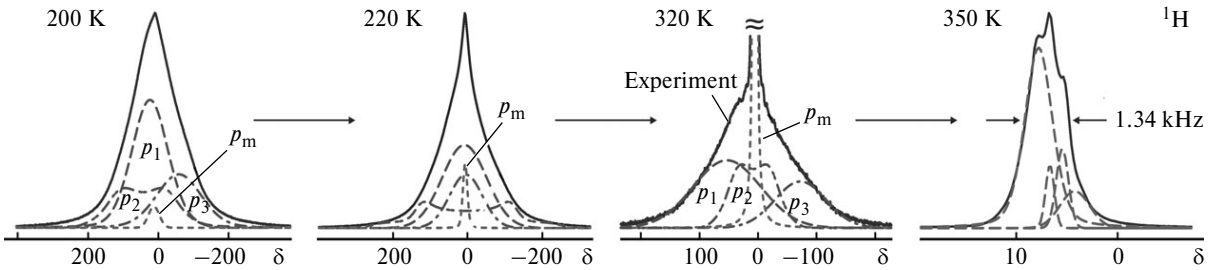

Fig. 8. ^{1}H NMR spectra of compound $(C_3H_8NO_3)Sb_2F_7$ at different temperatures (with Me_4Si as reference).

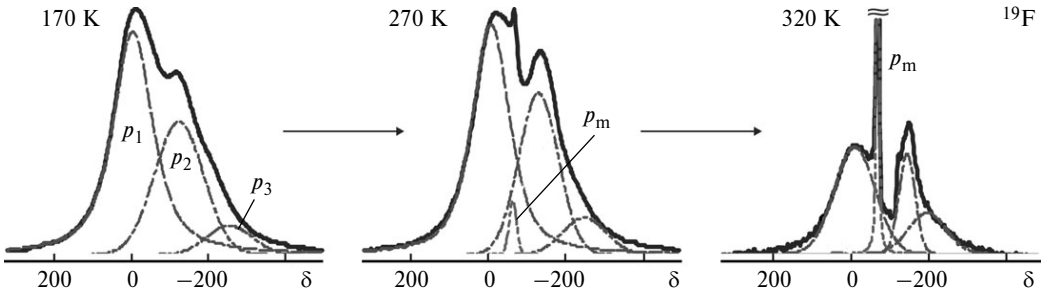

Fig. 9. Simulation of ^{19}F NMR spectra of compound $(C_3H_8NO_3)Sb_2F_7$ at different temperatures (with CCl_3F as reference).

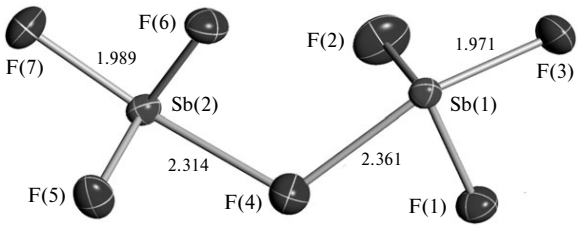

Fig. 10. Structure of complex anion $[Sb_2F_7]^-$.

mobile fluorine ions ($E_a \approx 0.43$ eV). As the temperature increases to 350 K, this component narrows to 2 kHz while its RII increases owing to a decrease in the RII of other spectral components and becomes as high as about 50% at 350 K. The appearance of mobile fluorine ions (diffusion) is due to the onset of fast exchange between different positions of fluorine atoms in the anion as temperature increases from 260 to 350 K, which is confirmed by almost constant (within the limits of the simulation error) position of the "center of gravity" of the triplet low-temperature NMR spectrum and by the CS of the component p_m: $\langle\delta\rangle = 1/7[4 \cdot (-7) + 2 \cdot (-120) + (-207)] = -67.8$ ppm. These data with certainty point to intramolecular dynamics between different ligands in the fluoride sublattice.

NMR data for compound $(C_6H_{14}NO_2)SbF_4$, (LeuH)SbF_4

Triangular shape of the ^{1}H NMR spectrum of compound (LeuH)SbF_4 at 300 K is a result of superposition of the signals from proton-containing groups (CH_3, CH_2, CH, NH_3, COOH) in the L-leucinium cation; however, the large number of such groups complicates a correct simulation of the NMR spectrum (Fig. 11).[6] Besides, there are two types of $(C_6H_{14}NO_2)^+$ cations with different coordination of NH_3 groups owing to formation of hydrogen bonds of different stength.[25]

Above 340 K, the ^{1}H NMR spectra of (LeuH)SbF_4 exhibit a narrow component ($\Delta H_{1/2} = 4.5 \pm 0.2$ kHz) whose intensity increases with increasing temperature (see Fig. 11). The presence of this component is indicative of the appearance of mobile protons ($E_a \approx 0.54$ eV) which account for more than 20% of the total number of ^{1}H atoms in the proton subsystem at 400 K and about 42% at 420 K. The shape (primarily Lorentzian, by 90%) and width of the narrow component (~4.3 kHz) suggests the development of translational diffusion in the proton sublattice of the complex.

The unit cell of a (LeuH)SbF_4 crystal contains two crystallographically independent antimony atoms, Sb(1) and Sb(2), with different environment[25] (Fig. 12). The coordination polyhedron of the Sb(1) atom is a ψ-tetrahedron $Sb(1)F_3E$ formed by three fluorine atoms and the lone electron pair E of the antimony(III) ion. The Sb(2) atom in the structure of $(C_6H_{14}NO_2)SbF_4$ is surrounded by five fluorine atoms and the lone electron pair; as a result, the coordination polyhedron of Sb(2) is a ψ-octahedron $Sb(2)F_5E$.

The asymmetric ^{19}F NMR spectrum of (LeuH)SbF_4 at 300 K can be simulated using three resonance lines p_1, p_2, and p_3 at $\delta \approx 138$, 97, and 28 ppm, respectively, with a RII ratio of about 45 : 28 : 27 (Fig. 13). This is in reason-

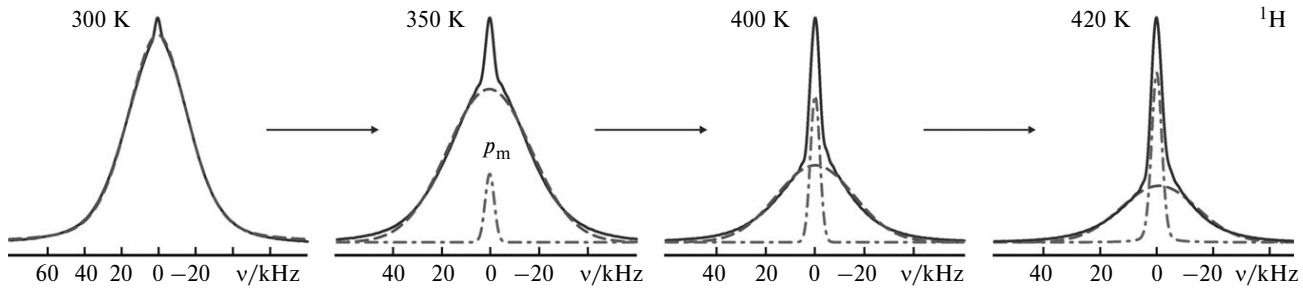

Fig. 11. Deconvolution of ^{1}H NMR spectra of compound (LeuH)SbF_4 at different temperatures.

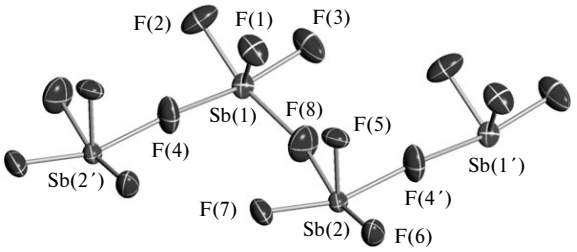

Fig. 12. Structure of complex anion $[SbF_4]_n^{n-}$ in compound $(LeuH)SbF_4$.[25]

able agreement with the distribution of fluorine atoms over structural positions (see Fig. 12).[24] A qualitative analysis of NMR data showed that the components p_1 and p_2 can correspond to fluorine atoms from the nearest environment of the antimony atoms Sb(2) and Sb(1) (5 + 3), while the component p_3 corresponds to three bridging fluorine atoms (Sb—F(8A), F(4), F(3B))[25] in the coordination polyhedron of the Sb(1) atom. This assignment is based on comparison of the CS values for the p_3 component (δ = 28 ppm), the p_2 component corresponding to the bridging fluorine atom F(3′) from the second coordination sphere of the antimony atom in $SbF_3 \cdot$ Leu (δ = ~25 ppm), and the p_2 component corresponding to the bridging fluorine atoms in $2SbF_3 \cdot (C_2H_5NO_2)$ (δ = 40 ppm). At $T > 320$ K, the ^{19}F NMR spectra of $(LeuH)SbF_4$ exhibit a narrow component p_m ($\Delta H_{1/2} < 3$ kHz) with $\delta = 96.5$ ppm; the intensity of this line increases with increasing temperature (Fig. 13). This implies the appearance of mobile fluorine ions. Since in the crystal structure of $(LeuH)SbF_4$ the $[SbF_4]_n^{n-}$ anions form polymer chains $[Sb_2F_8]_n^{2n-}$ composed of Sb_2F_8 dimers (see Fig. 12) comprising the SbF_3 and SbF_5 groups linked by the bridging fluorine atoms F(4) and F(8),[25] one can assume that raising the temperature causes the onset of reorientational motions of these groups. As a result, the fluoride bridges can be broken with "release" of a free fluorine ion and its migration along the chain.[37] Also, it cannot be ruled out that the mechanism of the appearance of highly mobile fluorine ions is related to the onset of fast exchange between different lattice sites occupied by fluorine atoms at $T > 320$ K. A possible confirmation is provided by the fact that the chemical shift of the p_m component within the limits of determination corresponds to the position of the "center of gravity" of the ^{19}F NMR spectrum for the "rigid" lattice $\langle\delta\rangle = 1/11(5 \cdot 138 + 3 \cdot 97 + 3 \cdot 28) = 101.4$ ppm.

In the temperature range of 383—415 K the DTA trace of $(LeuH)SbF_4$ exhibits an endothermic effect at 405 K, which corresponds to a PT. It can be due to either orientational disordering in both sublattices (this is typical of compounds containing complex anions, cations, or molecular groups[38]) or structural rearrangements. The newly formed $(LeuH)SbF_4$ polymorph is unstable and undergoes transformation to the molecular complex $SbF_3 \cdot$ Leu with time.

Among the known complexes of antimony fluorides with AA, electrophysical measurements were carried out only for $(LeuH)SbF_4$. It was found that the specific conductivity of $(LeuH)SbF_4$ increases by more than four orders of magnitude in the temperature range 300—385 K. The phase transition of $(LeuH)SbF_4$ has a diffuse character, *i.e.*, the conductivity increases gradually rather than abruptly in the temperature range from 383 to 403 K. After the PT, the specific conductivity increases again by two orders of magnitude and reaches a value of $\sim 2.15 \cdot 10^{-5}$ S cm^{-1} at $T = 403$ K. No specific conductivity measurements were performed at higher temperatures because of ductility of the high-temperature phase. The activation energy of conductivity was not exactly determined; it was evaluated as being in the range of 0.92—1.04 eV.

NMR data for complex $SbF_3 \cdot (C_6H_{13}NO_2)$, $SbF_3 \cdot$ Leu

According to differential thermal analysis (DTA) data,[6] the molecular complex $SbF_3 \cdot$ Leu is stable to 450 K. The ^1H NMR spectrum of the complex at 300 K (Fig. 14) exhibits a single symmetric line representing the superposition of signals from proton-containing groups in the leucine molecule (CH_3, CH, CH_2, and NH_2). The fact that the NMR spectra retain their shape as well as slight narrowing in the temperature range 300—420 K show that no ion motions with frequencies higher than 10^4 Hz occur in the proton subsystem.

Raising the temperature in the range of 300—420 K has almost no effect on the character of the ^{19}F NMR

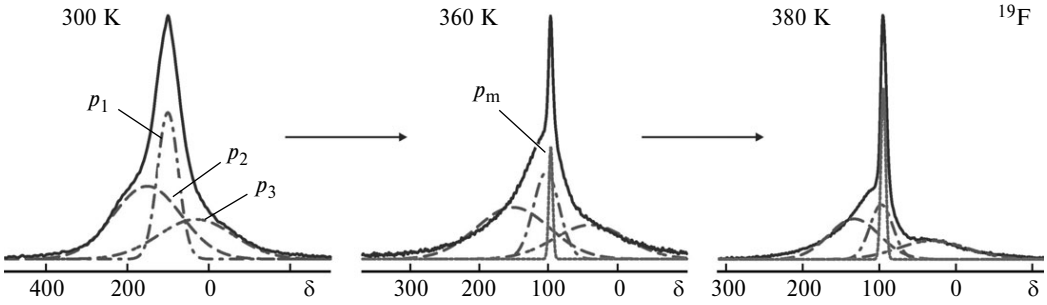

Fig. 13. ^{19}F NMR spectra of complex $(C_6H_{14}NO_2)SbF_4$ at different temperatures (with C_6F_6 as reference).

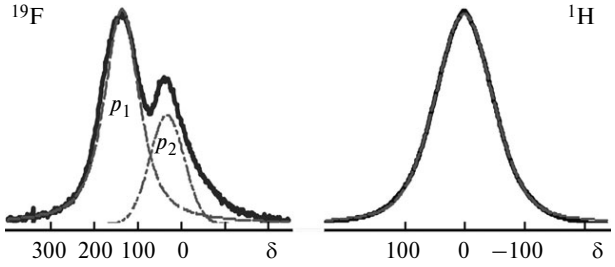

Fig. 14. ^{19}F NMR spectra (with C_6F_6 as reference) and ^{1}H NMR spectra (with Me_4Si as reference) of complex $SbF_3 \cdot$ Leu at 300 K.

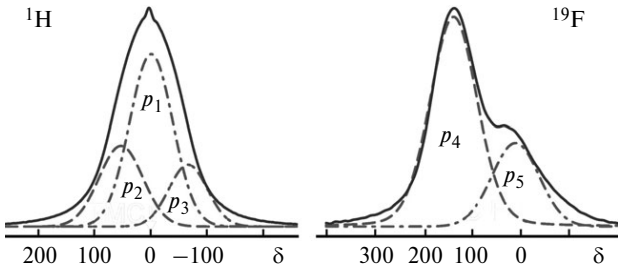

Fig. 15. ^{19}F NMR spectra (with C_6F_6 as reference) and ^{1}H NMR spectra (with Me_4Si as reference) of complex $SbF_3 \cdot$ Val at 300 K.

spectra of complex $SbF_3 \cdot$ Leu corresponding to the "rigid" lattice. The ^{19}F NMR spectrum at 300 K can be approximated using two components, p_1 and p_2 (see Fig. 14), with a RII ratio of 74 : 26. Taking account of the structure of the complex anion[24] (distorted octahedron SbF_3O_2E), the former component can be assigned to three fluorine atoms from the nearest environment of the antimony atom while the latter corresponds to the F(3′) atom from the second coordination sphere (Sb—F(3)′ distance is 2.8616 Å). The F(3)′ atom is used for pairwise connection of polymer chains into ribbons that form a 3D framework through the hydrogen bonds N—H···F and N—H···O.[24] This structure practically excludes the possibility for ion motions with frequencies higher than 10^4 Hz to occur.

NMR data for compound $SbF_3 \cdot (C_5H_{11}NO_2)$, $SbF_3 \cdot$ Val

Molecular complex $SbF_3 \cdot$ Val is stable to 423 K. At T = 475 K, the DTA trace exhibits an irreversible endothermic effect associated with melting of the compound and formation of X-ray amorphous product on cooling.[6] A qualitative analysis of the ^{19}F NMR spectra showed that the fluoride sublattice of the complex remains "rigid" throughout the temperature range studied ($S_2 \approx 43.5$ G^2). This suggests no fluorine ion transfer in the complex in the temperature range of 300—420 K. The asymmetric ^{19}F NMR spectrum of the compound at 300 K can be simulated using two lines, p_4 and p_5, with $\delta \approx 138$ and 18 ppm, respectively, and a RII ratio of ~74 : 26 (Fig. 15). This is in reasonable agreement with the distribution of fluorine atoms in the environment of the Sb(III) atom, *viz.*, three atoms from the first coordination sphere and one atom from the second coordination sphere (Sb—F bond length is 2.882 Å). The coordination polyhedron of the Sb(III) atom is a distorted octahedron SbF_3O_2E.[22]

An analysis of ^{1}H NMR spectra showed that the lineshape (see Fig. 15) and the second moment (25±1 G^2) remain almost unchanged as temperature increases from 300 to 400 K. It follows that no ion mobility also occurs in the proton subsystem of the complex $SbF_3 \cdot$ Val. The NMR spectra can be simulated using three Gaussian components p_1, p_2, and p_3 corresponding to the $2(CH_3)$, NH_3, and 2CH groups.

NMR data for compound $(C_2H_6NO_2)_3[InF_6]$, $(GlyH)_3[InF_6]$

According to ^{19}F NMR data (Figs 16 and 17), no ion motions with frequencies higher than 10^4 Hz occur in the fluoride sublattice of $(GlyH)_3[InF_6]$ in the temperature range of 150—250 K. At $T > 250$ K, the ^{19}F NMR spectra are narrowed (see Fig. 17). Taking account of the octahedral structure of the anion,[6] this can be related to the onset of reorientational motions of the complex anions $[InF_6]^{3-}$ about one or more symmetry axes. Isotropic reorientations in the fluoride sublattice of $(GlyH)_3[InF_6]$ probably become the main type of ion motions ($S_2 = 15 \rightarrow 5$ G^2) in the temperature range of 320—350 K. Note that anisotropic and isotropic reorientations of octahedral ions occur in all compounds containing them.[10,30—33]

Two «narrow» components ($\Delta H_{1/2}$ = 2.5—3 kHz) with the total RII of at most 5.5% appear in the ^{19}F NMR spectra (Fig. 18) at $T > 345$ K. The ^{19}F NMR spectrum at 370 K can be simulated using three components and the sum of the RII of the narrow lines is at most 21%. The lines with $\Delta H_{1/2} \approx 3$ kHz and $\Delta H_{1/2} = 2.5$ kHz (δ = 36 and 4 ppm, respectively) originate from the development of diffusion processes in the fluoride sublattice. The component with δ = 4 ppm probably corresponds to the mobile fluorine ions, while the line with $\Delta H_{1/2}$ = 17.5 kHz and δ = 2 ppm corresponds to fluorine atoms in the reorienting InF_6 octahedra. The assignment of the signal with CS = 36 ppm is ambiguous.

Two models were proposed[3] to describe diffusion in the fluoride sublattice of $(GlyH)_3[InF_6]$, *viz.*, diffusion of the entire complex anion InF_6^{3-} and successive hopping of individual F^- ions from one anion to another, which has a vacancy at the fluorine ion site in the octahedron.[10,39] In the latter case, the ion transport involves two types of atomic motions that occur successively. Hopping of fluorine ions from one octahedron to another and subsequent rotation of that polyhedron can be followed by a new hop of the fluorine ion towards the next InF_6 octahedron, *etc.*

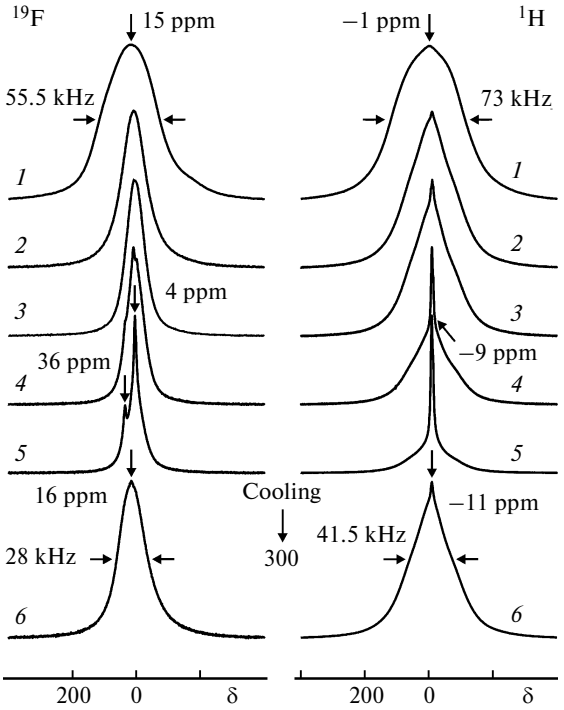

Fig. 16. ^{1}H NMR spectra (with Me_4Si as reference) and ^{19}F NMR spectra (with C_6F_6 as reference) of complex $(GlyH)_3[InF_6]$ at 150 (*1*), 300 (*2*), 335 (*3*), 350 (*4*), and 370 K (*5*) and on cooling from 370 to 300 K (*6*).

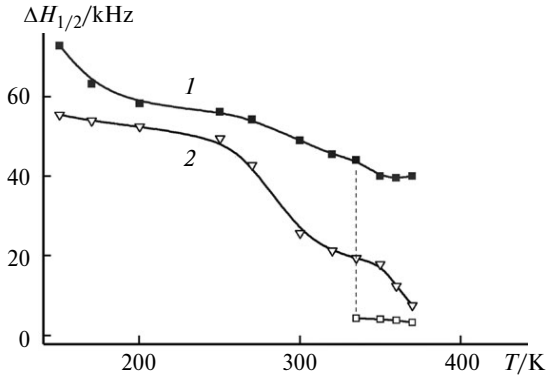

Fig. 17. Temperature dependences of the half-width of ^{1}H (*1*) and ^{19}F NMR spectra (E_a = 0.42 eV) (*2*) of compound $(C_2H_6NO_2)_3[InF_6]$.

Note that, according to NMR data obtained at 295 K, isotropic reorientations of NH_4^+ and TaF_6^- ions in NH_4TaF_6 are accompanied by long-distance diffusion of fluorine atoms.[40]

At 170 K, the ^{1}H NMR spectrum of $(GlyH)_3[InF_6]$ can be simulated using three components (Fig. 19). Two of them, p_1 and p_2, are the Pake doublets corresponding to NH_3 and CH_2 groups with RII of 39 and 33%, respectively, while the component p_3+p_1' with a total RII of 16.5 + 11.5 = 28.0 % corresponds to the COOH group and the central peak of the triplet from the NH_3 group in the glycinium cation. The splitting, Δ, of the doublet corresponding to the CH_2 group is 46±2 kHz and agrees with the inter-proton distance of 1.58±0.03 Å in this group. Evaluation of the Δ value in the doublet and the outermost components of the triplet from the NH_3 group gave a value of 84 kHz, which is comparable with the proton-proton distance in the NH_3 group (1.62 Å). The inter-proton distance in the CH_2 group (*e.g.*, in $CH_2Cl—CH_2Cl$ molecule), determined from the second moment (experiment and calculations),[41] is 1.69 Å (*cf.* 1.64 Å for the NH_3 molecule with the structure of a regular pyramid).

The experimental ^{1}H NMR spectrum of $(GlyH)_3[InF_6]$ at 335 K is simulated by two Pake doublets, a Gaussian line, and two close-lying narrow components p_m and p_x of width 2.3 and 1 kHz, respectively (Fig. 19), which is indicative of the appearance of mobile protons. Raising the temperature to 370 K has almost no effect on the RII of the p_x component (<2%), while the RII of the p_m component increases to 27%. A RII analysis of the components p_1, p_2, p_3, p_x, and p_m in the ^{1}H NMR spectrum of $(GlyH)_3[InF_6]$ simulated for T = 350 K showed that initially, the RII of the p_m component increases due to a decrease in the RII of the peaks p_1 and p_3+p_1', since the RII of the p_2 component corresponding to the CH_2 group remains almost unchanged. This trend in the changes in the RII of the spectral components also persists as the temperature increases to the maximum value of 370 K achieved in the experiment. Owing to highly probable reorientational motions of the NH_3 group around the C(2)—N bond (Fig. 20) one can assume that the appearance of mobile protons is related to a certain frequency of proton exchange between NH_3 and COOH groups that is

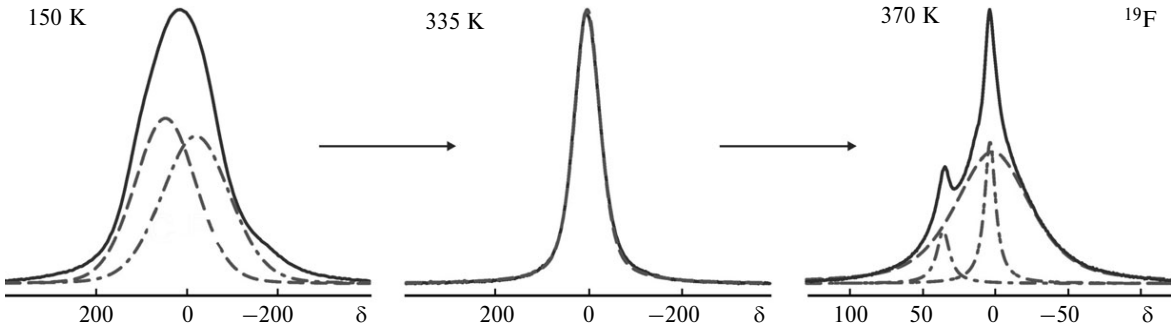

Fig. 18. ^{19}F NMR spectra of $(C_2H_6NO_2)_3[InF_6]$ at different temperatures (with C_6F_6 as reference).

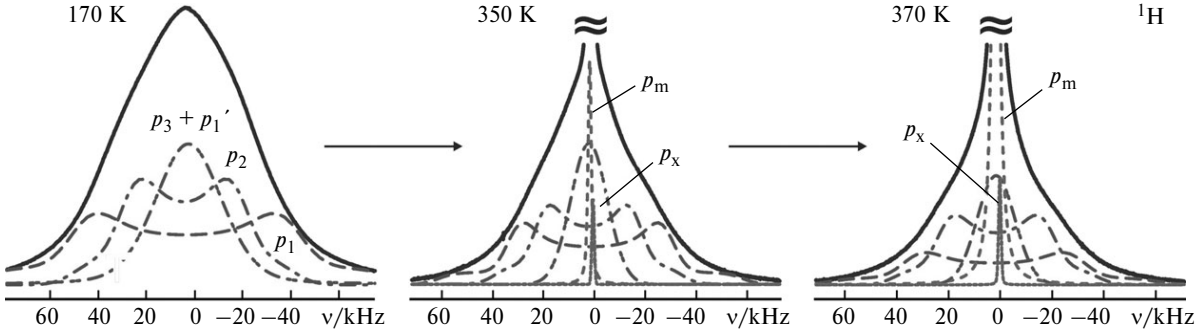

Fig. 19. ^{1}H NMR spectra of compound $(C_2H_6NO_2)_3[InF_6]$ at different temperatures (with Me_4Si as reference).

achieved on heating. The width (~2.5 kHz) and shape of the p_m component described by the Lorentzian function point to the development of translational diffusion in the proton subsystem, which occurs as migration of mobile protons in the crystal lattice. It is difficult to assign the weak p_x line (RII is about 1.5% at 370 K) to a particular atomic group; this line can even correspond to an impurity, whereas the p_m component corresponds to mobile protons in the glycinium cation.

According to DSC data, changes in the aggregation state of $(C_2H_6NO_2)_3[InF_6]$ occur at $T > 390$ K. In the temperature range of 220—430 K, the DSC trace exhibits an irreversible endothermic effect at 411 K, which corresponds to melting and formation of X-ray amorphous phase (XPA data) upon subsequent cooling of the sample (420 → 300 K).

Conclusion

We analyzed the NMR data for the amino acid complexes of antimony(III) and indium(III) fluorides and used them to determine the character of ion mobility in the compounds studied. The results of simulation of the low-temperature NMR spectra were corrected to be consistent with the structural data. It was shown that the character and types of ion mobility depend on the nature of the AA and on the structure of the complex compound. No ion mobility with frequencies higher than 10^4 Hz occurs in the fluoride and proton subsystems of the molecular complexes $SbF_3 \cdot Val$ and $SbF_3 \cdot Leu$ and in $(ValH)SbF_4 \cdot H_2O$ due to strong hydrogen bonding. Contrary to this, the complexes of antimony(III) fluorides and indium(III) fluoride with glycine, L-leucine $(C_6H_{14}NO_2)SbF_4$, and D,L-serine $(C_3H_8NO_3)Sb_2F_7$ are characterized by transition of ions in both subsystems from the "rigid" lattice to local motions (diffusion). The ^{19}F NMR spectra of the complexes of antimony(III) fluorides with AA where diffusion in the fluoride sublattice occurs demonstrate a characteristic feature, namely, an almost identical chemical shift of the p_m component corresponding to the mobile fluorine ions ($\delta = 97 \pm 3$ ppm). Thus, detection of this component is related to the onset of ligand exchange in the fluoride sublattice irrespective of the structure of the complex. Nevertheless, the exchange onset temperature depends on the structure of the fluoride sublattice. Possible mechanisms of the onset of ion mobility in both sublattices of the compounds in question were studied. A common feature of the complexes in hand is the formation of X-ray amorphous phase upon a PT followed by melting. The possibility for translational diffusion to occur in the entire fluoride (or proton) sublattice is limited by relatively low temperatures at which changes in the aggregation state of the compounds are observed. Therefore, practical application of these compounds in electrochemical devices is hardly probable. Nevertheless, the conductivity of one complex increased by six orders of magnitude to nearly $2.15 \cdot 10^{-5}$ S cm^{-1} upon heating from 300 to 403 K. Thus, a final decision on application of the compounds under study as components of high-conducting functional materials can be made only after performing electrophysical studies.

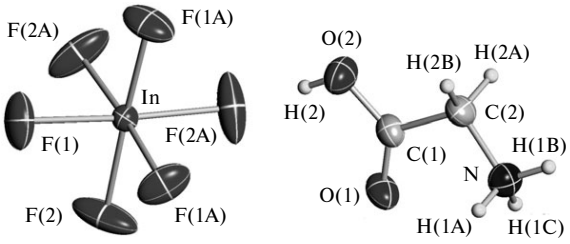

Fig. 20. Structure of anion and cation in compound $(C_2H_6NO_2)_3[InF_6]$.[3]

References

1. M. Fleck, A. M. Petrosyan, *Salts of Amino Acids: Crystallization, Structure and Properties*, Springer, Netherlands, Dordrecht, 2014.
2. G. Giester, V. V. Ghazaryan, M. Fleck, A. M. Petrosyan, *J. Fluor. Chem.*, 2017, **195**, 26.
3. V. Ya. Kavun, R. L. Davidovich, A. A. Udovenko, M. M. Polyantsev, V. B. Logvinova, *J. Fluor. Chem.*, 2018, **212**, 13.
4. R. L. Davidovich, V. B. Logvinova, L. A. Zemnukhova, A. A. Udovenko, I. P. Kondratyuk, *Sov. J. Coord. Chem.* (*Engl. Transl.*), 1991, **17**, 1342.

5. L. A. Zemnukhova, R. L. Davidovich, A. A. Udovenko, E. V. Kovaleva, *Russ. J. Coord. Chem.* (*Engl. Transl.*), 2005, **31**, 115.
6. V. Ya. Kavun, N. A. Didenko, N. V. Makarenko, A. B. Slobodyuk, E. B. Merkulov, N. F. Uvarov, L. A. Zemnukhova, *Russ. J. Inorg. Chem.* (*Engl. Transl.*), 2012, **57**, 1262.
7. N. V. Makarenko, V. Ya. Kavun, A. A. Udovenko, E. V. Kovaleva, L. A. Zemnukhova, *J. Fluor. Chem.*, 2018, **213**, 56.
8. R. Gupta, M. Mathur, A. K. Swami, J. Sharma, Y. Singh, *J. Saudi Chem. Soc.*, 2017, **21**, 67.
9. M. Lehmann, A. Schulz, A. Villinger, *Eur. J. Inorg. Chem.*, 2012, 822.
10. V. Ya. Kavun, V. I. Sergienko, *Diffuzionnaya podvizhnost´ i ionnyj transport v kristallicheskikh i amorfnykh ftoridakh elementov IV gruppy i sur´my(III)* [*Diffusion Mobility and Ion Transport in Crystalline and Amorphous Fluorides of Group IV Elements and Antimony (III)*], Dalnauka, Vladivostok, 2004, 298 pp. (in Russian).
11. L. A. Zemnukhova, R. L. Davidovich, *Z. Naturforsch. A*, 1998, **53**, 573.
12. R. Mary Jenila, I. Vetha Potheher, M. Vimalan, T. R. Rajasekaran, *J. Mater. Sci.: Mater. Electron.*, 2015, **26**, 6419.
13. E. Chacko, S. M. Linet, C. M. N. Priya, C. Vesta, B. M. Boaz, S. J. Dhas, *Indian J. Pure Appl. Phys.*, 2006, **44**, 260.
14. P. Rawat, S. K. Saroj, J. Kaur, R. Nagar, *J. Luminec.*, 2019, **210**, 392.
15. C. Besky Job, K. Ganesan, J. Benet Charles, *Der Pharma Chemica*, 2011, **3**, No. 6, 41.
16. M. P. Borzenkova, F. V. Kalinchenko, A. V. Novoselova, A. K. Ivanov-Schits, N. I. Sorokin, *J. Inorg. Chem. USSR* (*Engl. Transl.*), 1984, **29**, 703.
17. Y. N. Moskvich, B. I. Cherkasov, A. M. Polyakov, A. A. Sukhovskii, R. L. Davidovich, *Phys. Status Solidi (b)*, 1989, **156**, 615.
18. K. Yamada, Y. Ohnuki, H. Ohki, T. Okuda, *Chem. Lett.*, 1999, **28**, 627.
19. V. Ya. Kavun, N. F. Uvarov, A. B. Slobodyuk, O. V. Brovkina, L. A. Zemnukhova, V. I. Sergienko, *Russ. J. Electrochem.* (*Engl. Transl.*), 2005, **41**, 488.
20. C. Besky Job, R. T. Ananth Kumar, S. Paulraj, *Optik*, 2016, **127**, 55.
21. A. A. Udovenko, L. A. Zemnukhova, E. V. Kovaleva, R. L. Davidovich, *Russ. J. Coord. Chem.* (*Engl. Transl.*), 2005, **31**, 225.
22. A. A. Udovenko, N. V. Makarenko, E, V. Kovaleva, L. A. Zemnukhova, *J. Struct. Chem.* (*Engl. Transl.*), 2018, **59**, 1653.
23. A. A. Udovenko, R. L. Davidovich, L. A. Zemnukhova, E. V. Kovaleva, N. V. Makarenko, *J. Struct. Chem.* (*Engl. Transl.*), 2010, **51**, 540.
24 A. A. Udovenko, N. V. Makarenko, R. L. Davidovich, L. A. Zemnukhova, E. V. Kovaleva, *J. Struct. Chem.* (*Engl. Transl.*), 2010, **51**, 765.
25. A. A. Udovenko, N. V. Makarenko, R. L. Davidovich, L. A. Zemnukhova, E. V. Kovaleva, *J. Struct. Chem.* (*Engl. Transl.*), 2010, **51**, 904.
26. A. A. Udovenko, N. V. Makarenko, R. L. Davidovich, L. A. Zemnukhova, E. V. Kovaleva, *J. Struct. Chem.* (*Engl. Transl.*), 2011, **52**, 616.
27. V. Ya. Kavun, A. A. Udovenko, A. B. Slobodyuk, N. V. Makarenko, E. V. Kovaleva, L. A. Zemnukhova, *J. Fluor. Chem.*, 2019, **217**, 50.
28. L. A. Zemnukhova, T. A. Babushkina, T. P. Klimova, N. V. Makarenko, E. V. Kovaleva, *Russ. J. Gen. Chem.* (*Engl. Transl.*), 2014, **214**, 918.
29. S. E. Ashbrook, D. M. Dawson, *Nucl. Magn. Reson.*, 2016, **45**, 1.
30. A. G. Lundin, E. I. Fedin, *YaMR-spektroskopiya* [*NMR Spectroscopy*], Nauka, Moscow, 1986, 224 pp. (in Russian).
31. R. Youngman, *Materials*, 2018, **11**, 476.
32. S. P. Gabuda, Yu. V. Gagarinskiy, S. A. Polishchuk, *YaMR v neorganicheskikh ftoridakh* [*NMR in Inorganic Fluorides*], Atomizdat, Moscow, 1978, 205 pp. (in Russian).
33. G. Scholz, T. Krahl, M. Ahrens, C. Martineau, J. Y. Buzaré, C. Jäger, E. Kemnitz, *J. Fluor. Chem.*, 2011, **132**, 244.
34. W. Levason, M. E. Light, S. Maheshwari, G. Reid, W. Zhang, *Dalton Trans.*, 2011, **40**, 5291.
35. V. Ya. Kavun, A. B. Slobodyuk, M. M. Polyantsev, L. A. Zemnukhova, *J. Struct. Chem.* (*Engl. Transl.*), 2013, **54**, 137.
36. V. Ya. Kavun, A. A. Udovenko, N. V. Makarenko, L. A. Zemnukhova, A. B. Podgorbunskii, *J. Struct. Chem.* (*Engl. Transl.*), 2016, **57**, 658.
37. V. Ya. Kavun, A. V. Gerasimenko, V. I. Sergienko, R. L. Davidovich, N. I. Sorokin, *Russ. J. Appl. Chem.* (*Engl. Transl.*), 2000, **73**. 1025.
38. N. G. Parsonage, L. A. K. Staveley, *Disorder in Crystals*, Oxford, Clarendon University Press, 1978.
39. B. I. Cherkasov, Yu. N. Moskvich, A. A. Sukhovskii, R. L. Davidovich, *Phys. Solid State* (*Engl. Transl.*), 1988, **30**, 1652 [*Fizika tverdogo tela*, 1988, **30**, 1652].
40. T. Merle, J. P. Laval, B. Frit, J. Senegas, G. Grimberg, J. Strahle, *Eur. J. Solid State Inorg. Chem.*, 1994, **31**, 463.
41. H. S. Gutowsky, G. E. Pake, *J. Chem. Phys.*, 1950, **18**, 162.

Received September 20, 2019;
in revised form December 20, 2019:
accepted April 24, 2020